Non-iterative Parallel Transmission RF Pulse Design with Strict Temperature Constraints

Cem M. Deniz[1,2], Giuseppe Carluccio[1,2], Daniel K. Sodickson[1,2], and Christopher M. Collins[1,2]

[1]*Center for Advanced Imaging Innovation and Research (CAI2R), Department of Radiology, New York University School of Medicine, New York, NY, United States,* [2]*The Sackler Institute of Graduate Biomedical Sciences, New York University School of Medicine, New York, NY, United States*

TARGET AUDIENCE: Researchers who are interested in parallel transmission RF pulse design with consideration of RF heating.

INTRODUCTION: RF safety of subjects is generally ensured during parallel transmission (pTx) RF pulse design using SAR as a metric, as defined in international guidelines. Several optimization methods are employed for designing pTx RF pulses using strict SAR constraints[1,2]. Even though SAR provides easy tracking of RF deposition, temperature is a much more relevant parameter for subject safety. Recently, an iterative pTx RF pulse design approach has been proposed for a 3D time-of-flight sequence imposing strict temperature constraints by updating strict SAR constraints based on temperature simulations at each iteration[3]. In the present study, we propose a non-iterative parallel transmission RF pulse design approach which makes use of pre-computed temperature correlation matrices to impose strict temperature constraints.

METHODS: At each spatial location **r**, temperature correlation matrices[4], **T**, of a multi-channel RF transmit system were obtained from electromagnetic (EM) field simulations using the local electric field correlation matrices, **Q**, as a source term in Pennes' bioheat equation (Eq.1) for a specific sequence length T_{end}. The concept of virtual observation points (VOPs)[5] was incorporated in order to replace complete **T** matrices with a smaller number of constructed matrices, with VOPs $\mathbf{Z}^j$ j=1,...,N (N: the number of VOPs <<M: the number of voxels in the EM field simulation) designed to provide an acceptable overestimation of temperature.

Local Electric Field to Temperature Correlations (Eq.1)

$$\mathbf{Q}(\mathbf{r}) = \begin{bmatrix} \cdots & \cdots & \cdots \\ \cdots & Q_{mn}(\mathbf{r}) = \dfrac{\sigma(\mathbf{r})}{2}\left(e^{(m)}(\mathbf{r})\right)^{*} \cdot \left(e^{(n)}(\mathbf{r})\right) & \cdots \\ \cdots & \cdots & \cdots \end{bmatrix}_{LxL}$$

$$\xrightarrow[\text{Simulations}]{\text{Temperature}} \mathbf{T}(\mathbf{r}) = \begin{bmatrix} \cdots & \cdots & \cdots \\ \cdots & T_{mn}(\mathbf{r}) & \cdots \\ \cdots & \cdots & \cdots \end{bmatrix}_{LxL}$$

$$where\ \rho(\mathbf{r})C(\mathbf{r})\frac{\partial T_{mn}(\mathbf{r})}{\partial t} = \nabla\cdot\left(k\nabla T_{mn}(\mathbf{r})\right) - W(r)\rho_{bl}C_{bl}T_{mn}(\mathbf{r}) + \rho(\mathbf{r})Q_{mn}(\mathbf{r})$$

RF Pulse Optimization (Eq.2)

$$\tilde{\mathbf{b}}_{\mathrm{full}} = argmin\|\mathbf{A}_{\mathrm{full}}\mathbf{b}_{\mathrm{full}} - \mathbf{m}_{\mathrm{des}}\|_2^2$$

$$such\ that\ \alpha\mathbf{b}_{\mathrm{full}}^{H}\mathbf{Z}_{\mathrm{full}}^{j}\mathbf{b}_{\mathrm{full}} \le localTemperatureLimit \quad \forall j$$

$$where\ \mathbf{Z}_{\mathrm{full}}^{j} = \begin{bmatrix} \mathbf{Z}^j & & 0 \\ & \ddots & \\ 0 & & \mathbf{Z}^j \end{bmatrix}_{PLxPL}$$

Strict temperature constraints were incorporated into a small-tip-angle pTx RF pulse design by using the convex inequalities as constraints (Eq. 2), where $\mathbf{b}_{\mathrm{full}}=[\mathbf{b}^{T}_{1\Delta t}\ \ldots\ \mathbf{b}^{T}_{P\Delta t}]^{T}$ is the concatenation of coil RF pulse waveforms, $\mathbf{b}_{p\Delta t}=[b^{(1)}_{p\Delta t}\ \ldots\ b^{(L)}_{p\Delta t}]^{T}$, from L transmit channels at time $p\Delta t$ and $\alpha = \Delta t$ / TR. In addition to the constraints involving temperature predictions for a specific T_{end}, system related constraints such as individual channel forward and reflected peak and average power can be incorporated using calibrated power correlation matrices[6].

We can solve Eq. 2 using a range of efficient strategies for convex optimization since **T** matrices are positive definite and the defined constraints are quadratic convex functions. Similar to previous RF pulse design approaches,[1,6] a least-squares projection strategy was employed for the optimization problem, using, specifically, a Lanczos algorithm with Gram-Schmidt re-orthogonalization steps[7]. The SeDuMi[8] v1.2.1 solver, interfaced with YALMIP[9], was used to solve the reduced basis convex optimization problem.

In the present feasibility study, we performed EM field simulations (xFDTD 6.6, Remcom Inc., PA, USA) of a head-sized 8 element transmit array using the HUGO numerical model with 5 mm^3 resolution at 7T (Fig. 1). A constant rate spiral-in excitation *k*-space trajectory was used with duration=3.4ms, excitation resolution=2.5mm, sampling interval=10μs, maximum gradient slew rate=150mT/m/s and gradient amplitude=40mT/m. Parallel excitation RF pulses for uniform 17° excitation in a 2D rectangular region on the center axial slice were designed by solving Eq. 2. Temperature correlation matrices for each location, M= 48566 voxels, were calculated for 6 minutes (T_{end}) of gradient-echo based sequence with TR=9 ms. **T** matrices were then replaced by 25 VOPs, **Z,** in RF pulse design enabling a predefined 5% overestimation of the temperature at each subvolume. The local temperature limit on the constraint was defined as an increase of 1° Celsius.

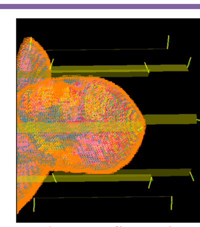

Figure 1: EM field simulation setup: 8 channel transmit array and HUGO model. Shield not shown.

RESULTS: Desired 2D excitation profile and axial flip angle maps resulting from RF pulses designed with and without strict temperature constraints are shown in Fig. 2. The excitation fidelity, the local maximum temperature, and the 10g SAR were reduced by using strict temperature constraints during the RF pulse design. The 6% decrease in excitation fidelity resulted in a slight overall flip angle decrease on the Bloch simulation results. The maximum local 10g SAR was 5.2 W/kg for the temperature constrained design, as opposed to 7.3 W/kg for the unconstrained design.

Desired Profile | **Unconstrained** | **Temperature Constrained**

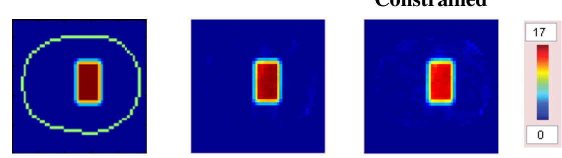

	Unconstrained	Temperature Constrained
Local maximum temperature increase (°C)	1.4	1.0
Maximum 10g SAR (W/kg)	7.3	5.2
NRMSE (%)	5.6	12.5

Figure 2: Top: Desired profile on an axial slice and Bloch simulation results of RF pulses calculated with and without temperature constraints. Bottom: Local maximum temperature and 10g SAR results with NRMSE of the excitation are written below images. The periphery of the head is indicated with a green line.

DISCUSSION: We demonstrated that calculated **T** matrices facilitate non-iterative design of parallel RF transmission pulses. Calculation of **T** matrices needs to be performed prior to RF pulse calculations with predefined T_{end} and short TR. To the extent that the **T** matrices used match the true tissue characteristics *in vivo*, using predefined temperature limits in pTx RF pulse design will ensure a safe MR scan. This RF design process with **T** matrices is fully capable of enforcing different temperature increase limits for different parts of the body, e.g. in the eyes. In this study, we have incorporated limits on local temperature increase in the RF pulse design. Similarly, limits on the absolute temperature can easily be incorporated into the RF pulse design by adding the maximum of pre-determined equilibrium temperature with no SAR to each VOP cluster in the constraints. We plan to incorporate this approach to short-TR SAR-limited 3D GRE-based hip microarchitecture scans at high field strengths[10]. This type of sequence should benefit from the proposed RF pulse design with temperature constraints as opposed to the existing SAR constraints[3].

REFERENCES: [1] Brunner DO, et al. (2010) MRM 63: 1280-91. [2] Lee J et al. (2012): MRM 67: 1566-78. [3] Boulant N et al. (2013) MRM 72: 679-88. [4] Carluccio G et al, (2015) ISMRM submitted. [5] Eichfelder G et al. (2011) MRM p1468-76. [6] Deniz CM et al. (2013): ISMRM 76. [7] Golub GH, et al. (1996) JHU Press: Matrix Computations. [8] Sturm, JF (1997) PhD Thesis, Tilburg University. [9] Lofberg, J. (2004) CACSD: 284-289. [10] Chang G et al. (2014) MRM p1384-93.